Diabetologia (2018) 61:2398–2411
https://doi.org/10.1007/s00125-018-4699-7

ARTICLE

Human fetoplacental arterial and venous endothelial cells are differentially programmed by gestational diabetes mellitus, resulting in cell-specific barrier function changes

Silvija Cvitic[1] · Boris Novakovic[2] · Lavinia Gordon[2] · Christine M. Ulz[1] · Magdalena Mühlberger[1] · Francisca I. Diaz-Perez[1] · Jihoon E. Joo[2] · Vendula Svendova[3] · Michael G. Schimek[3] · Slave Trajanoski[4] · Richard Saffery[2] · Gernot Desoye[1] · Ursula Hiden[1]

Received: 16 January 2018 / Accepted: 26 June 2018 / Published online: 8 August 2018

Abstract

Aims/hypothesis An adverse intrauterine environment can result in permanent changes in the physiology of the offspring and predispose to diseases in adulthood. One such exposure, gestational diabetes mellitus (GDM), has been linked to development of metabolic disorders and cardiovascular disease in offspring. Epigenetic variation, including DNA methylation, is recognised as a leading mechanism underpinning fetal programming and we hypothesised that this plays a key role in fetoplacental endothelial dysfunction following exposure to GDM. Thus, we conducted a pilot epigenetic study to analyse concordant DNA methylation and gene expression changes in GDM-exposed fetoplacental endothelial cells.

Methods Genome-wide methylation analysis of primary fetoplacental arterial endothelial cells (AEC) and venous endothelial cells (VEC) from healthy pregnancies and GDM-complicated pregnancies in parallel with transcriptome analysis identified methylation and expression changes. Most-affected pathways and functions were identified by Ingenuity Pathway Analysis and validated using functional assays.

Results Transcriptome and methylation analyses identified variation in gene expression linked to GDM-associated DNA methylation in 408 genes in AEC and 159 genes in VEC, implying a direct functional link. Pathway analysis found that genes altered by exposure to GDM clustered to functions associated with 'cell morphology' and 'cellular movement' in healthy AEC and VEC. Further functional analysis demonstrated that GDM-exposed cells had altered actin organisation and barrier function.

Conclusions/interpretation Our data indicate that exposure to GDM programs atypical morphology and barrier function in fetoplacental endothelial cells by DNA methylation and gene expression change. The effects differ between AEC and VEC, indicating a stringent cell-specific sensitivity to adverse exposures associated with developmental programming in utero.

Data availability DNA methylation and gene expression datasets generated and analysed during the current study are available at the National Center for Biotechnology Information (NCBI) Gene Expression Omnibus (GEO) database (http://www.ncbi.nlm.nih.gov/geo) under accession numbers GSE106099 and GSE103552, respectively.

Keywords Actin organisation · DNA methylation · Fetoplacental endothelial cells · Gestational diabetes mellitus · Programming

Gernot Desoye and Ursula Hiden contributed equally to this work.

Electronic supplementary material The online version of this article (https://doi.org/10.1007/s00125-018-4699-7) contains peer-reviewed but unedited supplementary material, which is available to authorised users.

✉ Ursula Hiden
ursula.hiden@medunigraz.at

[1] Department of Obstetrics and Gynecology, Medical University of Graz, Auenbruggerplatz 14, 8036 Graz, Austria

[2] Cancer and Disease Epigenetics, Murdoch Children's Research Institute, Royal Children's Hospital, Melbourne, VIC, Australia

[3] Institute for Medical Informatics, Statistics and Documentation, Medical University of Graz, Graz, Austria

[4] Center for Medical Research, Medical University of Graz, Graz, Austria

Research in context

What is already known about this subject?

- Gestational diabetes mellitus (GDM) programs the fetus in the long term and increases the risk for cardiovascular diseases in later life
- The diabetic environment affects endothelial function

What is the key question?

- Does maternal GDM program fetoplacental endothelial function?

What are the new findings?

- GDM alters actin organisation of fetoplacental arterial endothelial cells in the long term by changing DNA methylation and expression of genes involved in this pathway

How might this impact on clinical practice in the foreseeable future?

- Knowledge of programming processes may lead to changes in treatment and metabolic control among women with GDM and their offspring

Abbreviations

AEC	Arterial endothelial cells
dAEC	AEC from GDM pregnancies
DMR	Differentially methylated region
dVEC	VEC from GDM pregnancies
EBM	Endothelial basal medium
FC	Fold change
FDR	False discovery rate
GDM	Gestational diabetes mellitus
PCA	Principal component analysis
VEC	Venous endothelial cells

Introduction

Adverse insults during intrauterine life can induce long-term changes in the physiology and metabolism of the offspring and, thus, program future health. This phenomenon is referred to as fetal programming [1, 2]. Epigenetic mechanisms, including DNA methylation, are characterised by a high degree of plasticity and responsiveness to environmental stimuli [3] and are considered to play a key role in fetal programming. Indeed, altered DNA methylation in response to the environment in utero leads to gene expression changes and consequently affects placental function [4, 5].

Gestational diabetes mellitus (GDM) is a pregnancy-related glucose intolerance causing maternal and fetal hyperglycaemia [6]. As with other types of diabetes, GDM is a growing problem and affects ~15% of pregnancies worldwide [7]. Although GDM resolves after birth, it is associated with long-term adverse consequences for mother and offspring (i.e. an increased risk for later diabetes in the mother and development of features of the metabolic syndrome, including cardiovascular disease, in the offspring) [8, 9].

Accumulating evidence linking intrauterine exposures to later risk of cardiovascular disease has raised interest in the process of vascular development and its programming by adverse maternal environments, such as GDM. Being directly exposed to the altered metabolic milieu of GDM, the endothelial compartment of the fetoplacental unit represents an ideal tissue for investigating the role of epigenetics due to adverse environments in programming cardiovascular/metabolic function [1, 10]. This notion is further supported by the observation that endothelial and vascular dysfunction [11] are among the most prominent long-term consequences of diabetes and hyperglycaemia.

The vascular system is comprised of two major types of blood vessels, arterial and venous, which differ in various physiological and anatomical factors, reflecting their distinct functions. The identity of arterial endothelial cells (AEC) and venous endothelial cells (VEC) is associated with distinct gene expression signatures established early in development [12]. Epigenetic mechanisms, including DNA methylation, are key to specifying such differences [13]. We previously demonstrated widespread DNA methylation differences in essential endothelial genes in fetoplacental AEC and VEC [14]. Importantly, the distinct phenotypical characteristics of these cells were maintained after isolation and during in vitro culture [15].

Here we hypothesised that the altered intrauterine environment associated with GDM modifies DNA methylation of endothelial cells of the fetoplacental unit in a cell-type-specific (AEC vs VEC) manner and aimed to identify the relationship between genome-wide methylation and gene expression in fetoplacental endothelial cells from healthy and GDM-complicated pregnancies. We conducted a pilot study

to identify concordant gene methylation and expression changes induced by GDM, performed pathway analysis to identify functions and pathways subject to epigenetic dysregulation by GDM and tested a subset of these using functional studies.

Methods

Sample collection Ethical approval was obtained from the Medical University Graz (25-008ex12/13 and 27-268ex14/15). All women participating in the study provided written informed consent. Control placentas were collected from pregnancies of non-smoking (self-reported) women who had a negative 75 g OGTT performed at 25–28 weeks of gestation and were free from medical disorders or pregnancy complications. GDM was diagnosed according to WHO/IADPSG criteria [16]. The women who had a positive OGTT were either recommended a diet and classified as GDM A1 or were additionally treated with insulin (NovoRapid plus Insulatard; Novo Nordisk Pharma, Vienna, Austria) and classified as GDM A2. Control and GDM samples were matched for ethnicity and fetal sex, but not for maternal BMI, since being overweight is major risk factor for GDM. However, neither BMI nor gestational weight gain differed between control and GDM groups. In addition, the mean and median cell passage of primary cells from control and GDM women was similar. We also performed covariate analysis on multiple factors (gestational age, cord blood insulin, fetal weight and length, fetal ponderal index, placental weight, maternal C-reactive protein [CRP], maternal height, maternal weight and BMI before pregnancy and before birth and maternal gestational weight gain) using Bioconductor package limma (https://bioconductor.org/packages/release/bioc/html/limma.html) and identified an effect on a total of 27 CpG sites at 21 genes (electronic supplementary material [ESM] Table 1), representing only a small subset of total differentially methylated positions and suggesting that observed effects are a result of GDM. We should note, however, that the sample size is too small for such covariate analysis.

We used different samples for expression and methylation analysis. Analysis of RNA and DNA from the same sample would have resulted in better correlation but analysis of different samples, though matched for clinical variables and passages, gives more robust results. Table 1 shows maternal, neonatal and placental characteristics of expression and methylation analyses.

Cell culture Primary AEC and VEC were isolated from third-trimester human placentas after healthy and GDM-complicated pregnancies following a standard protocol [15]. Cells were characterised by immunocytochemical analysis [17] and cultured on 1% (vol./vol.) gelatin-coated flasks (75 cm^2) using endothelial basal medium (EBM; Cambrex Clonetics, Baltimore, MD, USA) supplemented with the EGM-MV BulletKit (Cambrex Clonetics). Cell isolations were used up to passage ten as no phenotypical change or altered responses of the cells to culture were observed.

DNA methylation analysis DNA (1 μg) isolated from fetoplacental AEC ($n = 9$), VEC ($n = 9$), AEC from GDM pregnancies (dAEC) ($n = 5$) and VEC from GDM pregnancies (dVEC) ($n = 9$), obtained from nine control and nine GDM placentas in total, was bisulphite converted using MethylEasy Bisulphite Modification Kit (Human Genetic Signatures, Sydney, NSW, Australia). Conversion efficiency was assessed by bisulphite-specific PCR (not shown). Hybridisation of bisulphite-treated samples to Illumina Infinium Human Methylation450 (HM450) BeadChips (Illumina, San Diego, CA, USA) was performed according to the manufacturer's instructions. Based on power calculations for the HM450 array, our sample size would allow us to detect changes of $\Delta\beta > 0.2$ and p value <0.05 [18]. The BeadChips were scanned using Illumina iScan (Illumina) and raw data were exported as IDAT files. Minfi Bioconductor package (https://bioconductor.org/packages/release/bioc/html/minfi.html) [19] imported data into R (version R 2.15.1), performed quality control, pre-processing and normalisation using the subset-quantile within array normalisation (SWAN) method [20]. The limma package [21] was used to fit a linear model to compare dAEC and dVEC vs control samples, with patient as random effect and allowing for batch effects. False discovery rate (FDR) was calculated by the Benjamini–Hochberg method. M values were calculated after removing probes on the sex chromosomes to eliminate potential sex bias and poor-performing probes. β values were derived from intensities defined by the ratio of methylated (M) to unmethylated (U) probes given by $\beta = M / (U + M + 100)$. For details of quality control, outlier identification and HM450 platform validation using locus-specific SEQUENOM MassARRAY EpiTYPER (Agena Bioscience, San Diego, CA, USA) [22], see ESM Methods and ESM Figs 1–3. For information on whether CpGs are located in differentially methylated regions (DMRs), see ESM Table 2 and for a discussion of advantages vs disadvantages of the HM450 platform, see ESM Methods. Unadjusted and adjusted p values and information on whether CpGs are located at potential SNPs, within topological domains (TADs) published in HUVECs [23] or part of a DMR, are given in the lists of significantly methylated CpGs available on Gene Expression Omnibus (GEO) database account GSE106099 (www.ncbi.nlm.nih.gov/geo).

RNA isolation Total RNA was isolated with RNeasy mini Kit (Qiagen, Hilden, Germany) and quality was assessed using a BioAnalyzer BA2100 (Agilent, Foster City, CA, USA) with

Table 1 Maternal, neonatal and placental clinical variables for gene expression and DNA methylation analyses

Variable	Gene expression		DNA methylation	
	Normal pregnancy	GDM pregnancy	Normal pregnancy	GDM pregnancy
Maternal data				
No. of individuals used for cell isolation	8	14	9	9
No. of cell isolations (AEC/VEC)	8/8	10/11	9/9	9/5
Age (years)	34.0 ± 7.3	32.8 ± 7.9	28.4 ± 6.3	32.7 ± 6.6
Gestational age (weeks)	39.6 ± 1.5	38.9 ± 1.2	40.8 ± 1.5	39.2 ± 1.3*
Height (m)	1.66 ± 0.09	1.66 ± 0.06	1.70 ± 0.04	1.70 ± 0.05
Weight before pregnancy (kg)	77.3 ± 17.5	83.0 ± 16.6	75.0 ± 11.6	83.6 ± 18.5
BMI before pregnancy	27.7 ± 3.8	30.1 ± 5.6	25.8 ± 3.1	28.6 ± 7.6
Weight before birth (kg)	92.8 ± 20.0	95.1 ± 18.1	90.2 ± 11.5	94.6 ± 17.6
BMI before birth	33.3 ± 4.3	34.8 ± 5.8	30.1 ± 4.9	33.0 ± 6.6
Gestational weight gain (kg)	15.5 ± 4.2	12.1 ± 9.6	15.2 ± 2.7	10.9 ± 10.3
CRP (nmol/l)	99 ± 87	56 ± 49*	92 ± 88	54 ± 52
HbA_{1c} (mmol/mol)	ND	38.8 ± 2.2	ND	37.7 ± 2.3
HbA_{1c} (%)	ND	5.7 ± 0.2	ND	5.6 ± 0.2
OGTT glucose (mmol/l)				
Fasting	4.35 ± 0.44	5.11 ± 0.42*	4.35 ± 0.23	5.56 ± 0.66*
1 h	6.33 ± 0.96	10.20 ± 1.91*	6.23 ± 1.14	9.32 ± 2.33*
2 h	5.64 ± 0.63	7.05 ± 1.45*	5.33 ± 0.73	6.35 ± 1.54*
GDM classification (A1/A2)		9/5		4/5
Neonatal data				
Male/female ratio	4/4	6/8	4/5	4/5
Offspring weight (g)	3547 ± 428	3275 ± 409	3443 ± 482	3318 ± 365
Offspring length (cm)	51.0 ± 2.1	50.4 ± 2.0	50.4 ± 2.7	50.6 ± 2.7
Placental weight (g)	515 ± 190	620 ± 188	619 ± 195	595 ± 159
Fetal ponderal index	26.7 ± 2.0	25.5 ± 2.2	26.8 ± 2.6	25.9 ± 4.6
Fetus/placenta weight ratio	6.25 ± 1.37	5.72 ± 1.74	5.89 ± 1.44	6.02 ± 1.78
Cord blood insulin (pmol/l)	ND	223 ± 269	150 ± 177	181 ± 285
Cord blood C-peptide (nmol/l)	ND	1.06 ± 0.93	ND	0.60 ± 0.23
Cell culture data				
Cell isolation passage	6.1 ± 1.2	6.6 ± 1.1	5.4 ± 1.0	4.8 ± 0.6

Data are presented as means ± SD

The ethnicity was similar in all groups

*$p < 0.05$ by Student's t test vs respective control group

ND, not determined

the RNA 6000 Nano LabChip Kit (Agilent). Samples with an RNA Integrity Number ≥8.5 were further used.

Microarray gene expression analysis Total RNA from AEC ($n = 8$) and VEC ($n = 8$) isolated from eight placentas from normal pregnancies and dAEC ($n = 11$) and dVEC ($n = 10$) isolated from 14 placentas from pregnancies complicated by GDM was labelled using Ambion WT Expression Kit for Affymetrix GeneChip Whole transcript (WT) Expression Arrays (Life Technologies, Carlsbad, CA). The cRNA was hybridised to GeneChip Human 1.0 ST arrays according to the manufacturer's instructions (Affymetrix, Santa Clara, CA, USA). Washing and staining (GeneChip HT Hybridization, Wash and Stain Kit; Affymetrix) was performed with Affymetrix GeneChip fluidics station 450. Arrays were scanned using Affymetrix GeneChip scanner GCS3000. Labelling and hybridisation controls were evaluated with Affymetrix Expression Console EC 1.1. Data were analysed with RMA (robust multi-chip average), including background correction, quantile normalisation, $\log_2$ transformation and median polish summarisation using Genomic Suite v6.5 (Partek, St Louis, MO, USA) [24]. Statistical analysis used one-way ANOVA with fetal sex and mother as random factors. The p values were adjusted for multiple testing

using the Benjamini–Hochberg method (R/Bioconductor package 'multtest'; https://www.bioconductor.org/packages/release/bioc/html/multtest.html) [25, 26].

qPCR cDNA was synthesized from 50 ng total RNA of different cell isolations ($n = 10$ per group) then used for microarray analysis according to protocol (SuperScript II Reverse Transcriptase protocol; Invitrogen, Carlsbad, CA, USA). qPCR was performed with TaqMan gene expression assays (Applied Biosystems, Carlsbad, CA, USA) and ABI Prism 5700 Sequence Detection System (Applied Biosystems, Foster City, CA, USA). The mean hypoxanthine-guanine phosphoribosyltransferase 1 (*HPRT1*) and ribosomal protein L30 (*RPL30*) expression was used as internal control as their expression was unaffected by GDM (not shown). Data were analysed using the $2^{-\Delta\Delta C_t}$ method [27]. Statistical analysis used Student's t test in SigmaPlot (Systat Software, San Jose, CA, USA).

Pathway analysis Gene lists were analysed with Ingenuity Pathway Analysis (IPA, version 2.3) (Qiagen). Cut-off for methylation differences was $p < 0.05$ and $\Delta\beta \geq 0.2$ and for gene expression $p < 0.05$ and fold change (FC) ≥1.5. When investigating pathways the cut-off was set to $\Delta\beta \geq 0.1$ (methylation) and FC ≥1.3 (expression) in order to have sufficient genes for the analysis.

F-actin immunofluorescence staining AEC ($n = 5$), VEC ($n = 6$), dAEC ($n = 5$) and dVEC ($n = 5$), each in quadruplicates, were seeded in gelatin-coated chamber slides (50,000 cells/well). Participants' characteristics are provided in ESM Table 3. After 24 h, slides were transferred to room temperature, washed with HBSS and fixed with 3.7% (wt./vol.) formaldehyde in PBS for 10 min. After washing with PBS, cells were permeabilised with 0.1% (vol./vol.) Triton X-100 in PBS for 25 min, washed with PBS, blocked with 1% (wt./vol.) BSA in PBS for 25 min and incubated phalloidin-488 FITC (1:20, Thermo Fisher, Eugene, OR, USA) with DL550 (DyLight 550 goat-anti mouse, 1:100, Thermo Fisher) for 1 h in the dark. Stained cells were washed with PBS and slides were mounted with Dako fluorescent mounting medium (Dako, Carpinteria, CA, USA) with DAPI (1:2000). After overnight drying, actin organisation was observed using a Zeiss LSM 510 Meta microscope, objective Plan-Apochromat 63×/1.4 Oil DIC, at 495 nm and 518 nm excitation wavelength (Zeiss, Oberkochen, Germany) using Zeiss LSM Image Browser. F-actin staining was performed and photographed by a blinded observer.

Electrical cell-substrate impedance sensing Impedance measurements were performed using an electrical cell-substrate impedance sensing (ECIS) system (Applied Biophysics, Troy, NY, USA) [28]. AEC ($n = 10$) and dAEC ($n = 6$) (80,000 cells/well), VEC ($n = 8$) and dVEC ($n = 4$) (110,000 cells/well) were seeded in 400 μl EBM on gelatin-coated gold electrodes (8W10E+ arrays; Applied Biophysics), in duplicates. Participants' characteristics are provided in ESM Table 3. VEC are smaller in diameter and were seeded in higher density. Thus, both AEC and VEC reached confluency after 12 h. Impedance was then recorded at 4 kHz for 24 h. Linear mixed-effect model using R package nlme (https://CRAN.R-project.org/package=nlme) was fitted for AEC and VEC separately. GDM, time and the interaction between them were used as fixed effects. Time was also used as random effect.

Results

GDM alters the DNA methylation profile of fetoplacental AEC and VEC To analyse changes in DNA methylation profile associated with exposure of fetoplacental AEC and VEC to GDM in utero (dAEC and dVEC), we measured the methylation of >450,000 CpG sites. Principal component analysis (PCA) of the entire methylation dataset demonstrated cell type (AEC vs VEC) as a main source of variation but also showed clear separation according to GDM status (Fig. 1a). Hierarchical clustering identified cell type as the greatest contributor to methylation variation (ESM Fig. 1) while high correlation between technical replicates indicated low inter-array variability (ESM Fig. 2).

Linear regression indicated that exposure to GDM influenced methylation levels ($p < 0.05$ and $\Delta\beta \geq 0.2$) at 2617 CpGs that annotated to 2063 genes in dAEC and 1568 CpGs that annotated to 1360 genes in dVEC (Fig. 1b). The lists of differentially methylated CpGs are deposited as Excel files at GEO database, accession number GSE106099. Not surprisingly given the sample size, these sites did not remain significant following FDR adjustment for multiple testing applied to control for false discoveries. Of the total differential methylation associated with GDM, 351 genes and 51 CpGs were common to both cell types. In contrast to dVEC, where variation was equally distributed between hyper- and hypomethylation, dAEC showed hypermethylation at only 33% of sites while 67% were hypomethylated (Fig. 1b). This was also reflected by a marginal decrease of overall DNA methylation (average methylation levels detected across all probes) with GDM, particularly in AEC, as illustrated by kernel density plot and methylation index (ESM Fig. 4a, b). The box plots and heat maps shown in ESM Fig. 5 illustrate global and gene-specific methylation differences in GDM-exposed cells in more detail.

Great distance analysis showed that most of the GDM-associated variation in CpG methylation occurs in the proximal region upstream of genes (−5 to 0 kb from the transcriptional start) (Fig. 1e, f) in both cell types. In contrast to this,

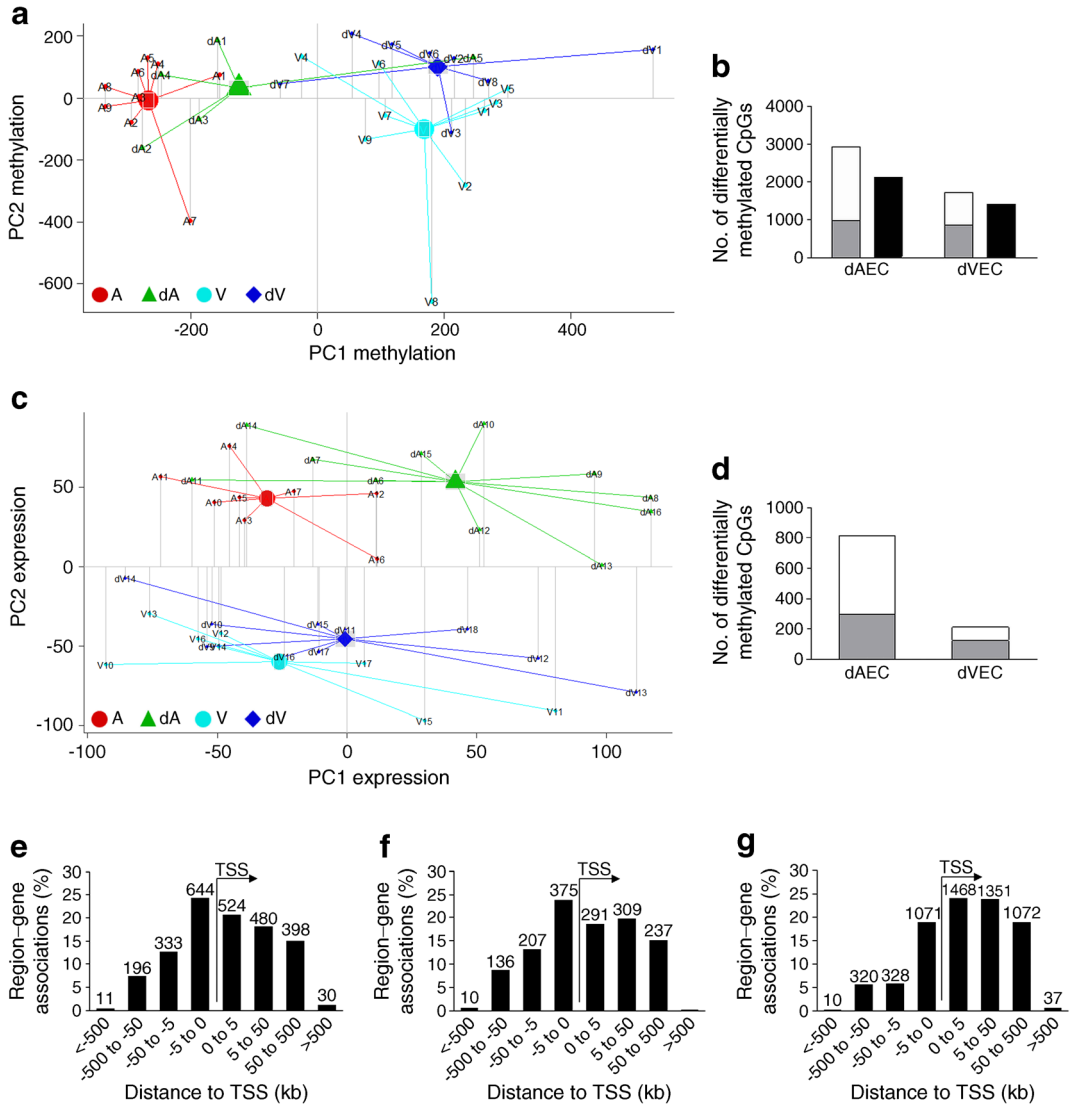

Fig. 1 (**a**, **c**) PCA plot of DNA methylation (**a**) and gene expression (**c**) arrays. The first (PC1) and second principal components (PC2) are shown on the *x*- and *y*-axis, respectively. (**b**, **d**) Number of differentially methylated CpGs (**b**) and number of associated genes (**d**) in fetoplacental AEC and VEC exposed to GDM (dAEC and dVEC, respectively) vs control cells using a cut-off of $p < 0.05$, $\Delta\beta \geq 0.2$ for methylation and $p < 0.05$, FC ≥1.5 for gene expression. In (**b**), the grey section of the bars indicates the number of hypermethylated CpGs, the white section of the bars indicates the number of hypomethylated CpGs and the black bars indicate the number of associated genes. In (**d**), the grey section of the bars indicates the number of upregulated genes and the white section of the bars indicates the number of downregulated genes. (**e**–**g**) Great distance analysis of altered CpG methylation relative to transcription start site (TSS). Associations for gene regions are shown for differentially methylated (hyper- and hypomethylated) CpGs in dAEC vs AEC (**e**) and dVEC vs VEC (**f**) ($p < 0.05$, $\Delta\beta \geq 0.2$) and for differentially methylated CpGs between AEC and VEC (**g**) ($p < 0.05$, $\Delta\beta \geq 0.4$). The absolute number of associated genes is indicated above each bar

cell-type-specific methylation (AEC vs VEC) is enriched downstream of the transcription start site (0 to 50 kb; Fig. 1g).

Locus-specific DNA methylation profiling of selected genes significantly correlated with genome-wide measurements ($r^2 = 0.83$ for arterial and $r^2 = 0.74$ for venous group) and thus validated the HM450 DNA methylation platform (ESM Fig. 3).

Pathways and functions of genes associated with altered methylation pattern in GDM Functional analysis of differentially methylated genes in dAEC and dVEC revealed that the molecular functions 'cellular function and maintenance' and 'cell morphology' were predominantly altered. Unique and cell-specific affected functions with a high number of target genes were 'cellular development' in dAEC and 'molecular transport' in dVEC (Table 2).

GDM alters gene expression profile of fetoplacental AEC and VEC PCA of the global transcriptome levels assessed at >30,000 transcripts in AEC and VEC clearly separated groups according to both cell type and GDM status (Fig. 1c). Unsupervised hierarchical clustering also discriminated AEC

Table 2 Top five significantly enriched molecular functions in Ingenuity Pathway Analysis for differentially methylated and top five for the differentially expressed genes in GDM-exposed AEC and VEC

Molecular function	*p* value	Score[a]
DNA methylation		
AEC		
Cellular function and maintenance	6.94×10^{-6} to 3.87×10^{-2}	176
Cellular assembly and organisation[b]	2.86×10^{-5} to 3.87×10^{-2}	114
Post-translational modification	1.54×10^{-4} to 3.77×10^{-2}	26
Cell morphology[b]	2.39×10^{-4} to 4.01×10^{-2}	92
Cellular development	2.39×10^{-4} to 4.40×10^{-2}	147
VEC		
Cellular function and maintenance	8.24×10^{-4} to 4.91×10^{-2}	53
Molecular transport	8.24×10^{-4} to 4.91×10^{-2}	51
Cell morphology[b]	9.34×10^{-4} to 4.58×10^{-2}	45
Cell-to-cell signalling and interaction	9.34×10^{-4} to 4.94×10^{-2}	48
Cellular compromise	9.34×10^{-4} to 2.89×10^{-2}	14
Gene expression		
AEC		
Cell cycle	8.42×10^{-22} to 1.26×10^{-2}	159
Cellular assembly and organisation[b]	8.42×10^{-22} to 1.11×10^{-2}	106
DNA replication, recombination and repair	8.42×10^{-22} to 1.11×10^{-2}	159
Cellular movement[b]	2.54×10^{-8} to 1.11×10^{-2}	89
Cellular growth and proliferation	1.03×10^{-6} to 1.15×10^{-2}	234
VEC		
Cell cycle	1.75×10^{-6} to 1.83×10^{-2}	48
Cell death and survival	4.96×10^{-5} to 1.36×10^{-2}	25
Cellular assembly and organisation[b]	7.46×10^{-5} to 1.67×10^{-2}	46
Cellular function and maintenance	7.46×10^{-5} to 1.67×10^{-2}	38
DNA replication, recombination and repair	7.46×10^{-5} to 1.74×10^{-2}	24

Genes significantly differentially methylated ($p < 0.05$; $\Delta\beta \geq 0.2$) or significantly differentially expressed ($p < 0.05$; FC ≥1.5) after GDM exposure in AEC and VEC, respectively, were enriched using Ingenuity Pathway Analysis. Molecular functions are comprised of multiple subcategories to which genes are assigned with different significance yielding a *p* value range (Fisher's exact test)

[a] Score represents the number of affected genes assigned to a specific molecular function

[b] Molecular functions related to cell morphology and actin organisation

from VEC, again highlighting the greatest influence of cell type. Furthermore, dAEC vs control AEC clustered, while there was no clear separation in the venous group (ESM Fig. 6). Analysis of genes significantly influenced by GDM ($p < 0.05$) with a ≥ 1.5-fold expression change, identified 812 genes in dAEC, with 36% being upregulated and 64% downregulated (Fig. 1d). In dVEC only 211 genes had changed expression, with 57% being upregulated and 43% downregulated (Fig. 1d). Interestingly, only 92 genes were commonly affected by GDM in both cell types. A list of the top 100 differentially expressed genes in dAEC and dVEC vs controls is available at the GEO database, accession number GSE103552. A subset of differentially expressed genes identified by microarray was validated by qPCR, confirming differential expression of six out of nine genes (ESM Table 4).

Pathways and functions of differentially expressed genes in GDM Molecular functions enriched with the differentially expressed genes in GDM were 'cell cycle', 'cellular assembly and organisation' and 'DNA replication, recombination and repair' in both AEC and VEC (Table 2), indicating a strong common effect of diabetes.

Concordant DNA methylation and expression changes in fetoplacental AEC and VEC To investigate the relationship between DNA methylation and gene expression, methylation and gene expression datasets were combined. For each CpG, differences in β values between control cells and GDM-exposed cells (Δβ) were calculated and compared with corresponding gene expression differences. Setting the cut-off in the significant methylation difference to ≥10% ($\Delta\beta \geq 0.1$) and in the gene expression to FC ≥1.3, concordant changes in

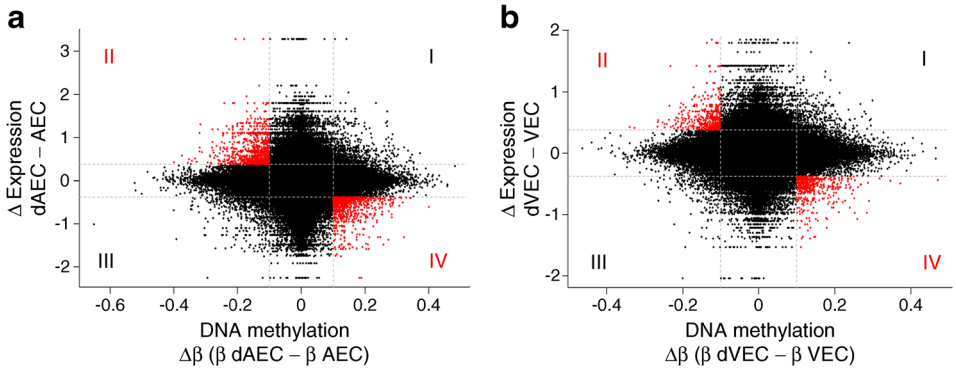

Quadrant	dAEC	No. CpGs	No. Genes
I	Hypermethylated Upregulated	152	101
II	Hypomethylated Upregulated	290	156
III	Hypomethylated Downregulated	267	205
IV	Hypermethylated Downregulated	118	92

Quadrant	dVEC	No. CpGs	No. Genes
I	Hypermethylated Upregulated	72	52
II	Hypomethylated Upregulated	117	74
III	Hypomethylated Downregulated	93	49
IV	Hypermethylated Downregulated	42	33

Fig. 2 Relationship between DNA methylation and gene expression changes associated with GDM in fetoplacental AEC and VEC. Scatterplot of DNA methylation (*x*-axis) and gene expression (*y*-axis) for HM450 probes with differences between control and GDM-exposed AEC (**a**) and VEC (**b**). Cut-offs are set to ≥10% ($\Delta\beta \geq 0.1$) methylation difference and to FC ≥1.3 in the gene expression. Points in red indicate genes likely to be under epigenetic regulation by DNA methylation, with increased methylation associated with decreased gene expression and vice versa. The tables below the scatterplots indicate the respective direction of methylation and gene expression changes as well as the number of affected CpGs and genes

DNA methylation and gene expression (hypermethylated – downregulated and hypomethylated – upregulated) were detected. In dAEC, 118 genes were hypermethylated and downregulated, while 290 genes were hypomethylated and upregulated (Fig. 2a). In dVEC, 42 genes were hypermethylated and downregulated, while 117 genes were hypomethylated and upregulated (Fig. 2b). Of all genes showing concordant methylation and expression change in GDM, only six were altered in dAEC and dVEC (Table 3).

Genes with concordant DNA methylation and gene expression change clustered to molecular functions involving actin reorganisation processes ('cell morphology' and 'cellular movement') in both dAEC and dVEC, with the largest number of affected molecules in 'cell morphology'. 'Carbohydrate metabolism', 'cell cycle' and 'cell-to-cell signalling and interaction' were also listed as molecular functions significantly influenced by GDM in both cell types (Table 4).

Table 3 Genes commonly regulated by GDM in AEC and VEC

Gene symbol	Gene name	Direction of expression and methylation change
EGFR	Epidermal growth factor receptor	Concordant in AEC and VEC
		Upregulated in AEC and downregulated in VEC
GABBR1	γ-Aminobutyric acid (GABA) B receptor, 1	Concordant in AEC and VEC
		Upregulated in AEC and VEC
LMF1	Lipase maturation factor 1	Concordant in VEC
		Upregulated in AEC and VEC
NCKAP5	NCK-associated protein 5	Concordant in AEC and VEC
		Upregulated in AEC and VEC
SKIL	SKI-like oncogene	Concordant in VEC
		Upregulated in AEC and VEC
SULF2	Sulfatase 2	Concordant in VEC
		Upregulated in AEC and VEC

The table shows genes significantly differentially methylated ($p < 0.05$; $\Delta\beta \geq 0.1$) and expressed ($p < 0.05$; FC ≥1.3) after GDM exposure in both AEC and VEC. Overlap was performed after integration of DNA methylation and gene expression data

Table 4 Top five significantly enriched molecular functions in Ingenuity Pathway Analysis for genes whose expression is potentially regulated by DNA methylation by GDM in AEC and VEC

Regulation	Molecular function	*p* value	Score[a]
AEC			
Hypomethylated/upregulated	Cell morphology[b]	5.79×10^{-7} to 1.63×10^{-2}	40
	Cellular movement[b]	2.54×10^{-5} to 1.56×10^{-2}	35
	Cell-to-cell signalling and interaction	5.75×10^{-5} to 1.63×10^{-2}	28
	Carbohydrate metabolism	1.98×10^{-4} to 1.63×10^{-2}	14
	Cellular development	1.98×10^{-4} to 1.63×10^{-2}	33
Hypermethylated/downregulated	Cell-to-cell signalling and interaction	2.18×10^{-5} to 4.61×10^{-2}	11
	Cellular compromise	2.18×10^{-5} to 1.82×10^{-2}	10
	Molecular transport	5.86×10^{-4} to 4.74×10^{-2}	10
	Cell cycle	7.69×10^{-4} to 4.86×10^{-2}	11
	Cellular assembly and organisation[b]	7.69×10^{-4} to 4.61×10^{-2}	16
VEC			
Hypomethylated/upregulated	Carbohydrate metabolism	4.55×10^{-5} to 1.17×10^{-2}	4
	Small molecule biochemistry	4.55×10^{-5} to 2.72×10^{-2}	11
	Cell morphology[b]	1.51×10^{-4} to 2.72×10^{-2}	23
	Cellular function and maintenance	1.51×10^{-4} to 2.62×10^{-2}	20
	Cell-to-cell signalling and interaction	1.58×10^{-4} to 2.72×10^{-2}	11
Hypermethylated/downregulated	Cell cycle	1.48×10^{-4} to 4.85×10^{-2}	4
	Protein synthesis	4.12×10^{-4} to 1.42×10^{-2}	6
	Cellular movement[b]	4.76×10^{-4} to 4.58×10^{-2}	3
	Cell death and survival	1.17×10^{-3} to 4.98×10^{-2}	5
	Cell morphology[b]	1.42×10^{-3} to 4.71×10^{-2}	4

Genes significantly differentially methylated ($p < 0.05$; $\Delta\beta \geq 0.1$) and differentially expressed ($p < 0.05$; FC ≥1.3) after exposure to GDM in AEC and VEC were enriched using Ingenuity Pathway Analysis. Molecular functions are comprised of multiple subcategories to which genes are assigned with different significance yielding a *p* value range (Fisher's exact test)

[a] Score represents the number of affected genes assigned to a specific molecular function

[b] Molecular functions related to cell morphology and actin organisation

Functional effects of GDM on actin organisation and barrier function To link pathway analysis results to cellular function, we investigated in vitro actin organisation in control and GDM-exposed cells. Phalloidin staining of F-actin (Fig. 3a) demonstrated that exposure to GDM differentially disrupted actin organisation in AEC. While in control AEC the actin cytoskeleton was organised in parallel actin bundles, the cytoskeleton was disorganised in dAEC. In VEC, GDM did not induce similar effects.

As the actin cytoskeleton is essential for maintaining the endothelial barrier, we further investigated barrier function. Real-time analysis of the electrical impedance of cell monolayers showed an increased average impedance of 16% in dAEC vs AEC ($p = 0.01$) (Fig. 3b). In contrast, GDM tended to reduce the average impedance of VEC by 30%, but without reaching significance ($p = 0.24$). These distinct effects of GDM on barrier function in AEC and VEC parallel the aforementioned differences in actin organisation.

Expression profile of genes involved in endothelial cell adhesion mirrors the effect of GDM on barrier function in fetoplacental AEC vs VEC Intercellular junction proteins join vascular endothelial cells and proteins of adherens junctions are most important for barrier function. Moreover, focal adhesions anchor endothelial cells to the basement membrane. Linker proteins such as vinculin and paxillin interconnect focal adhesions and intercellular junctions through the cytoskeleton. Their complex interplay in regulating actin organisation and vascular permeability is controlled by Rho GTPases [29]. We used expression levels of genes involved in focal adhesions, endothelial junctions and cytoskeleton rearrangement to generate a heatmap illustrating the effects of GDM on their expression in fetoplacental AEC and VEC (Fig. 4). This analysis revealed that GDM had the greatest effect on AEC, particularly on expression of focal adhesion-related genes: GDM upregulated various cellular integrins and extra cellular matrix genes, such as collagens and laminins, reflecting increased barrier function of dAEC potentially as a consequence of

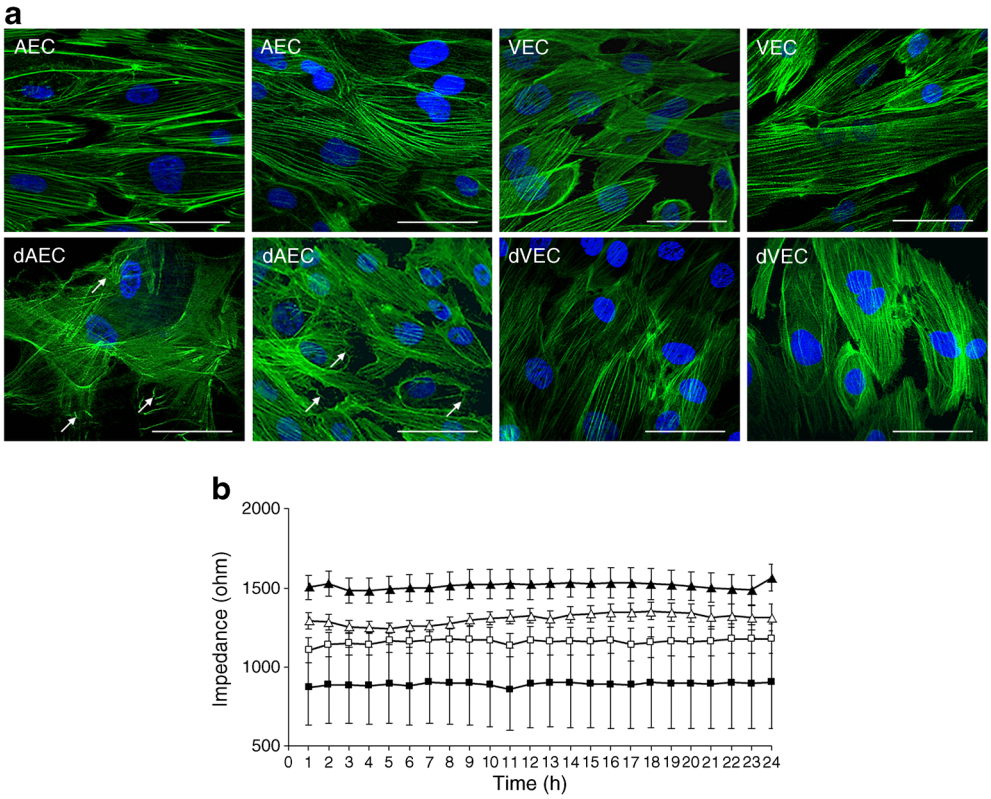

Fig. 3 Effect of GDM on F-actin organisation and barrier function. (**a**) F-actin fibres in primary fetoplacental AEC and VEC, after normal or GDM pregnancy were stained with phalloidin (green). Nuclei were stained with DAPI (blue). Note that AEC after normal pregnancy show a more organised actin fibre network, while the dAEC, exposed to GDM, reveal more cross-linked F-actin bundles. This difference was not found in the dVEC, exposed to GDM. Two representative stainings of $n = 5$ (AEC and dAEC) or $n = 6$ individual cell isolations (VEC and dVEC) per group are shown, each performed in quadruplicate. Original magnification ×400. Scale bar, 40 μm. White arrows indicate less organised actin fibres in dAEC. (**b**) Barrier function was assessed by real-time analysis of the electrical impedance of cell monolayers. After reaching maximum impedance, endothelial resistance of primary AEC and VEC, after normal ($n = 10$ and 8, respectively) or GDM pregnancy ($n = 6$ and 4, respectively), was followed over 24 h. Data are plotted as means ± SEM at 1 h intervals. Data were generated in three independent experiments for each cell type separately, in duplicate. For statistical comparison, a linear mixed-effects model was fitted, showing significantly increased average impedance in dAEC vs AEC ($p < 0.01$). Reduced average electrical impedance of dVEC was not significant ($p = 0.24$). White triangles, AEC; white squares, dAEC; black triangles, VEC; black squares, dVEC

enhanced attachment to extracellular matrix. Rho GTPases and their upstream regulators (i.e. Rho guanine nucleotide exchange factors) and downstream targets (i.e. *ROCK1*) were also altered in dAEC. Fewer of these genes were affected by GDM in VEC.

Discussion

The placenta is the largest vascular bed of the fetus. It is sensitive to exogenous exposures, reflected by the influence of diverse environmental stimuli on placental epigenetic marks, gene expression and function [5, 30]. The effect of GDM on DNA methylation has previously been investigated in total placental tissue [31–33]. However, the presence of distinct cell types complicates interpretation and calls for cell-type-specific approaches [5]. Furthermore, studies on the link between GDM-altered DNA methylation and resulting phenotypes have generally been limited to selected genes [34, 35]. The present study is the first attempt to delineate the effects of GDM on DNA methylation, transcription changes and functional consequences in offspring endothelium at the cellular level.

We report evidence that metabolic disturbances associated with GDM: (1) alter global DNA methylation and the gene expression profile of AEC and VEC; (2) have a cell-type-specific effect, with a greater number of genes affected in AEC than in VEC; and (3) affect genes involved in cell morphology, including those inducing cell-type-specific responses in actin organisation and barrier function.

GDM indeed altered DNA methylation and the gene expression profile of both AEC and VEC, supporting the concept of fetal metabolic programming by environmental stimuli. The individual signatures altered by GDM, however, differed between cells of arterial vs venous origin. Of the genes responsive to in utero exposure to GDM (as reflected by changes in DNA methylation and expression), only six were common to both AEC and VEC. These included *EGFR* and

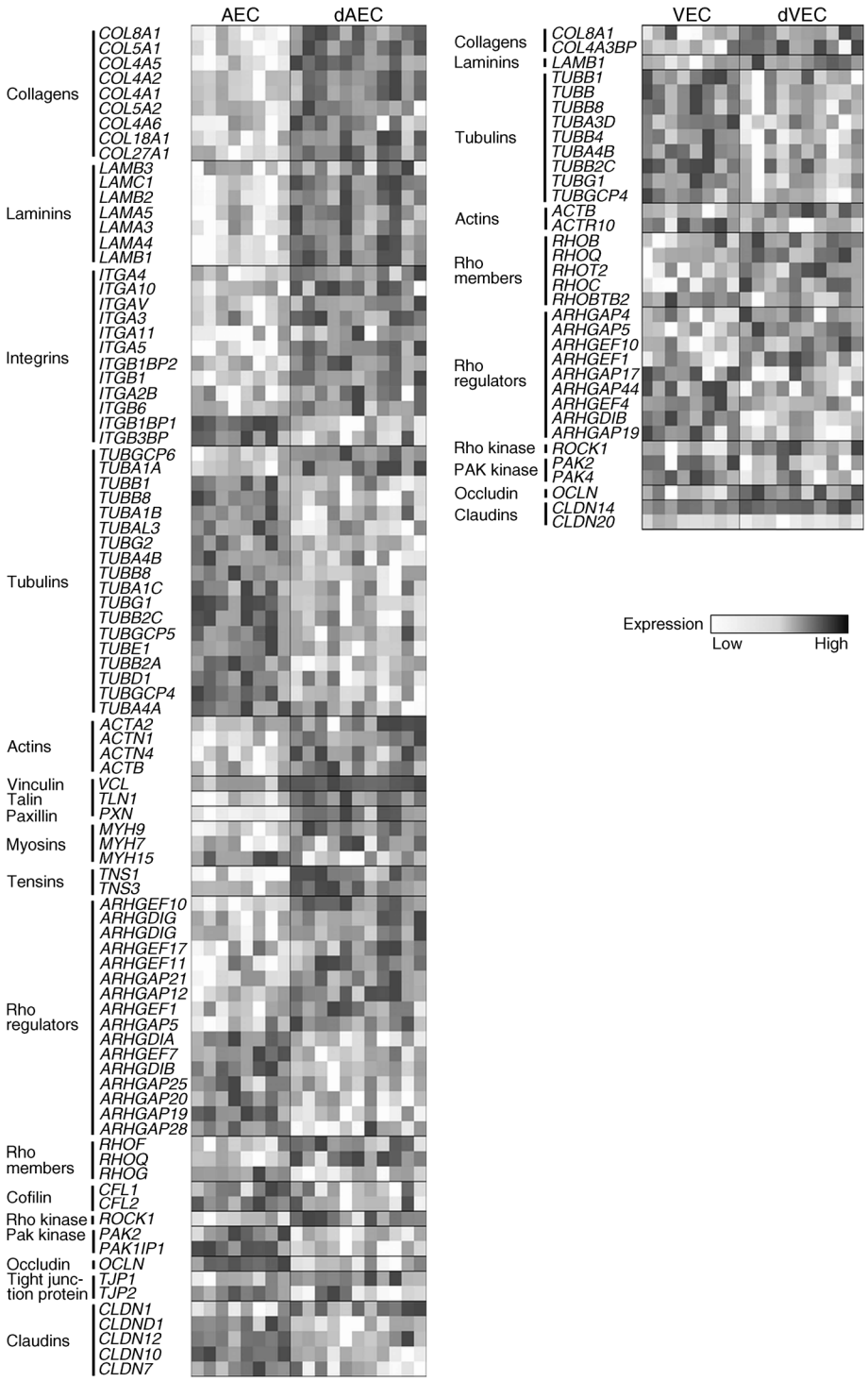

Fig. 4 Heat map of genes implicated in endothelial cell barrier function. The heat map depicts only genes that show significant expression difference ($p < 0.05$) in GDM-exposed endothelial cells vs control cells and that are related to focal adhesion, adherens and/or tight junctions, or cytoskeleton actin organisation. The colour bar indicates the expression of a particular gene from low (white) to high expression (black)

SULF2, encoding epidermal growth factor receptor and sulfatase 2, respectively, both linked to diabetic complications [36, 37]. The small number of genes commonly dysregulated by GDM in AEC and VEC strongly argues for cell-type-specific responses and metabolic programming of endothelial cells to the intrauterine environment. Indeed, VEC were less responsive to the GDM environment, as reflected by fewer CpGs and genes being affected, as compared with AEC. The reason for these cell-specific differences in susceptibility towards the GDM environment is unknown. Our previous studies showed that VEC are characterised by lower overall DNA methylation and a more juvenile phenotype than AEC [14, 15]. From this we speculated that VEC will be more amenable to the GDM-associated alterations. Moreover, differences in the two vascular loops with regard to the composition of cord blood constituents, blood flow and degree of oxygenation may play a

role. Importantly, the venous blood composition of the fetoplacental unit depends on net exchange of available substrates between mother and placenta, while arterial blood composition is influenced foremost by fetal metabolism [38, 39]. The intrinsic factors in parallel with the metabolic disturbances in arteries and veins in GDM [40, 41] may account for differences and susceptibility towards GDM programming. It has yet to be discovered which of the factors altered in GDM may be responsible for altered DNA methylation and subsequent programming of cell function. Although transient hyperglycaemia is sufficient to induce permanent epigenetic changes in endothelial cells [42], the potential contribution of other factors should not be neglected. Based on pathway analysis of concordantly regulated genes, we identified 'cell morphology' as a pathway altered by GDM in both AEC and VEC. However, a cell-type-specific effect of GDM on programming of AEC and VEC morphology was found by studying actin organisation, which was influenced foremost in AEC. This arterial–venous distinction in response to GDM was maintained when we analysed barrier integrity, which also depends on actin organisation: cell monolayer impedance was increased in GDM-exposed AEC, paralleled by an upregulation of genes involved in endothelial cell adhesion. Our finding that GDM environment affects endothelial cell morphology through DNA methylation is supported by a previous study reporting that pathways related to 'focal adhesion' were influenced by GDM in cord blood and placenta in women of South Asian origin [33]. Moreover, 'cell adhesion' was reported to be the most enriched cluster of GDM-affected genes in the placenta [32].

The precise consequences that altered actin organisation may have on endothelial cell function of macrovascular vessels in vivo can only be hypothesised. The actin cytoskeleton drives the adaption to shear stress and optimisation of cell shape in response to blood flow [43, 44]. Moreover, actin organisation and its tethering to adhesion complexes is essential for endothelial barrier function [45] and fluid infiltration, to which macrovascular endothelial cells significantly contribute [46].

We acknowledge several limitations of our study such as the small sample size. As in other omics studies with small sample size [26], none of the differential methylation remained statistically significant following FDR adjustment for multiple testing. This, however, does not exclude the potential for phenotype-specific associations but additional evidence is required to support a link. The main aim of this study was to identify biologically relevant functions rather than individual genes affected by GDM and we believe our strategy of using less-stringent criteria for pathway analysis is appropriate. Furthermore, probes with unadjusted p values of <0.05 were chosen and validated using other techniques, for both the Affymetrix and HM450 platforms. We further recognise that we have no information on the composition of cord blood or on vascular function in the offspring and future studies are needed in this regard.

We do not know whether the GDM-induced changes observed in AEC and VEC isolated from placenta are representative for the vasculature of other fetal organs. However, both are exposed to the same circulation, tempting us to speculate that this is a possibility. Support comes from studies in diabetic adults, which report disturbances in the expression of focal adhesion components [47] and integrins [48] which may influence endothelial cell shape and barrier function [49], in line with long-term effects of intrauterine programming by diabetic environment, at least for these specific processes. Further, in other adult tissues such as adipose, processes related to regulation of cytoskeleton and focal adhesions seem to be susceptible towards epigenetic regulation by diabetic environment [50].

In conclusion, this is the first study to identify cell-specific effects of GDM in human primary endothelial cells of arterial and venous origin from the same vascular loop. Furthermore, we are the first to link cell-type-specific genome-wide-scale DNA methylation and gene expression changes in GDM with a follow-up of functional consequences indicated by pathway analysis. The results of this study will hopefully stimulate further work associating programmed endothelial changes in the placenta with long-term vascular alterations in GDM-exposed offspring.

Acknowledgements Open access funding provided by Medical University of Graz. We would like to acknowledge the Division Core Facility for Molecular Biology at the Center for Medical Research at the Medical University of Graz for hybridisation of samples to the Affymetrix microarrays and the Australian Genome Research Facility (AGRF) for hybridisation of bisulphite-treated samples to Illumina Infinium Human Methylation450 (HM450) BeadChips.

Data availability DNA methylation and gene expression datasets generated and analysed during the current study are available at the National Center for Biotechnology Information (NCBI) Gene Expression Omnibus (GEO) database (http://www.ncbi.nlm.nih.gov/geo) under accession numbers GSE106099 and GSE103552, respectively.

Funding This work was supported by the European Union's Seventh Framework Programme (FP7/2007–2013) project EarlyNutrition under grant agreement no. 289346 and by the PhD programme Molecular Medicine from the Medical University Graz. RS and BN are supported by National Health and Medical Research Council (Australia) Fellowships and the Victorian Government Operational Infrastructure Support Scheme.

Duality of interest The authors declare that there is no duality of interest associated with this manuscript.

Contribution statement SC was responsible for the experimental design, carried out the experiments, performed data analysis and wrote the manuscript. LG performed most of the data analysis. BN and JEJ acquired and analysed data. CMU, MM and FIDP acquired data. VS and MGS performed data analysis. ST performed data analysis and data visualisation. RS, UH and GD designed the study and wrote the manuscript. All authors revised the manuscript and approved the final version. SC and UH are the guarantors of the work, have full access to all the data in the study and

take responsibility for the integrity of the data and the accuracy of the data analysis.

References

1. Friedman JE (2015) Obesity and gestational diabetes mellitus pathways for programming in mouse, monkey, and man-where do we go next? The 2014 Norbert Freinkel Award Lecture. Diabetes Care 38:1402–1411
2. Padmanabhan V, Cardoso RC, Puttabyatappa M (2016) Developmental programming, a pathway to disease. Endocrinology 157:1328–1340
3. Feil R, Fraga MF (2012) Epigenetics and the environment: emerging patterns and implications. Nat Rev Genet 13:97–109
4. Novakovic B, Sibson M, Ng HK et al (2009) Placenta-specific methylation of the vitamin D 24-hydroxylase gene: implications for feedback autoregulation of active vitamin D levels at the fetomaternal interface. J Biol Chem 284:14838–14848
5. Januar V, Desoye G, Novakovic B, Cvitic S, Saffery R (2015) Epigenetic regulation of human placental function and pregnancy outcome: considerations for causal inference. Am J Obstet Gynecol 213:S182–S196
6. Carpenter MW (2007) Gestational diabetes, pregnancy hypertension, and late vascular disease. Diabetes Care 30(Suppl 2):S246–S250
7. Chu SY, Callaghan WM, Kim SY et al (2007) Maternal obesity and risk of gestational diabetes mellitus. Diabetes Care 30:2070–2076
8. Wright CS, Rifas-Shiman SL, Rich-Edwards JW, Taveras EM, Gillman MW, Oken E (2009) Intrauterine exposure to gestational diabetes, child adiposity, and blood pressure. Am J Hypertens 22:215–220
9. Clausen TD, Mathiesen ER, Hansen T et al (2009) Overweight and the metabolic syndrome in adult offspring of women with diet-treated gestational diabetes mellitus or type 1 diabetes. J Clin Endocrinol Metab 94:2464–2470
10. Hanson M, Gluckman P (2005) Endothelial dysfunction and cardiovascular disease: the role of predictive adaptive responses. Heart 91:864–866
11. Haubner F, Lehle K, Munzel D, Schmid C, Birnbaum DE, Preuner JG (2007) Hyperglycemia increases the levels of vascular cellular adhesion molecule-1 and monocyte-chemoattractant-protein-1 in the diabetic endothelial cell. Biochem Biophys Res Commun 360:560–565
12. Swift MR, Weinstein BM (2009) Arterial-venous specification during development. Circ Res 104:576–588
13. Bennett-Baker PE, Wilkowski J, Burke DT (2003) Age-associated activation of epigenetically repressed genes in the mouse. Genetics 165:2055–2062
14. Joo JE, Hiden U, Lassance L et al (2013) Variable promoter methylation contributes to differential expression of key genes in human placenta-derived venous and arterial endothelial cells. BMC Genomics 14:475
15. Lang I, Schweizer A, Hiden U et al (2008) Human fetal placental endothelial cells have a mature arterial and a juvenile venous phenotype with adipogenic and osteogenic differentiation potential. Differentiation 76:1031–1043
16. International Association of Diabetes and Pregnancy Study Groups Consensus Panel, Metzger BE (2010) International association of diabetes and pregnancy study groups recommendations on the diagnosis and classification of hyperglycemia in pregnancy. Diabetes Care 33:676–682
17. Lang I, Pabst MA, Hiden U et al (2003) Heterogeneity of microvascular endothelial cells isolated from human term placenta and macrovascular umbilical vein endothelial cells. Eur J Cell Biol 82:163–173
18. Saffari A, Silver MJ, Zavattari P et al (2018) Estimation of a significance threshold for epigenome-wide association studies. Genet Epidemiol 42:20–33
19. Aryee MJ, Jaffe AE, Corrada-Bravo H et al (2014) Minfi: a flexible and comprehensive Bioconductor package for the analysis of Infinium DNA methylation microarrays. Bioinformatics 30:1363–1369
20. Maksimovic J, Gordon L, Oshlack A (2012) SWAN: subset-quantile within array normalization for illumina infinium HumanMethylation450 BeadChips. Genome Biol 13:R44
21. Ritchie ME, Phipson B, Wu D et al (2015) Limma powers differential expression analyses for RNA-sequencing and microarray studies. Nucleic Acids Res 43:e47
22. Ehrich M, Nelson MR, Stanssens P et al (2005) Quantitative high-throughput analysis of DNA methylation patterns by base-specific cleavage and mass spectrometry. Proc Natl Acad Sci U S A 102:15785–15790
23. Niskanen H, Tuszynska I, Zaborowski R et al (2018) Endothelial cell differentiation is encompassed by changes in long range interactions between inactive chromatin regions. Nucleic Acids Res 46:1724–1740
24. Downey T (2006) Analysis of a multifactor microarray study using Partek genomics solution. Methods Enzymol 411:256–270
25. Huber W, Carey VJ, Gentleman R et al (2015) Orchestrating high-throughput genomic analysis with Bioconductor. Nat Methods 12:115–121
26. Pollard K, Dudoit S, van der Laan M (2005) Multiple testing procedures: the multtest package and applications to genomics. In: Gentleman R, Carey VJ, Huber W, Irizarry RA, Dudoit S (eds) Anonymous bioinformatics and computational biology solutions using R and bioconductor. Statistics for biology and health. Springer, New York, pp 249–271
27. Livak KJ, Schmittgen TD (2001) Analysis of relative gene expression data using real-time quantitative PCR and the $2^{-\Delta\Delta C_t}$ method. Methods 25:402–408
28. Giaever I, Keese CR (1991) Micromotion of mammalian cells measured electrically. Proc Natl Acad Sci U S A 88:7896–7900
29. Yuan SY, Rigor RR (2010) Regulation of endothelial barrier function. Morgan & Claypool, San Rafael
30. Bouchard L, Hivert MF, Guay SP, St-Pierre J, Perron P, Brisson D (2012) Placental adiponectin gene DNA methylation levels are associated with mothers blood glucose concentration. Diabetes 61:1272–1280
31. Ruchat SM, Houde AA, Voisin G et al (2013) Gestational diabetes mellitus epigenetically affects genes predominantly involved in metabolic diseases. Epigenetics 8:935–943
32. Liu L, Zhang X, Rong C et al (2014) Distinct DNA methylomes of human placentas between pre-eclampsia and gestational diabetes mellitus. Cell Physiol Biochem 34:1877–1889
33. Finer S, Mathews C, Lowe R et al (2015) Maternal gestational diabetes is associated with genome-wide DNA methylation variation in placenta and cord blood of exposed offspring. Hum Mol Genet 24:3021–3029
34. El Hajj N, Pliushch G, Schneider E et al (2013) Metabolic programming of *MEST* DNA methylation by intrauterine exposure to gestational diabetes mellitus. Diabetes 62:1320–1328

35. Cheng X, Chapple SJ, Patel B et al (2013) Gestational diabetes mellitus impairs Nrf2-mediated adaptive antioxidant defenses and redox signaling in fetal endothelial cells in utero. Diabetes 62: 4088–4097
36. Hassing HC, Mooij H, Guo S et al (2012) Inhibition of hepatic sulfatase-2 in vivo: a novel strategy to correct diabetic dyslipidemia. Hepatology 55:1746–1753
37. Akhtar S, Benter IF (2013) The role of epidermal growth factor receptor in diabetes-induced cardiac dysfunction. BioImpacts 3:5–9
38. Nikischin W, Lehmann-Willenbrock E, Weisner D, Oldigs HD, Schaub J (1993) Comparison of umbilical arterial versus umbilical venous blood pH correlated with arterio-venous glucose difference and cardiotocographic score. Eur J Pediatr 152:840–843
39. Tea I, Le Gall G, Kuster A et al (2012) 1H-NMR-based metabolic profiling of maternal and umbilical cord blood indicates altered materno-foetal nutrient exchange in preterm infants. PLoS One 7: e29947
40. Taricco E, Radaelli T, Rossi G et al (2009) Effects of gestational diabetes on fetal oxygen and glucose levels in vivo. BJOG 116: 1729–1735
41. Ortega-Senovilla H, Schaefer-Graf U, Meitzner K et al (2011) Gestational diabetes mellitus causes changes in the concentrations of adipocyte fatty acid-binding protein and other adipocytokines in cord blood. Diabetes Care 34:2061–2066
42. El-Osta A, Brasacchio D, Yao D et al (2008) Transient high glucose causes persistent epigenetic changes and altered gene expression during subsequent normoglycemia. J Exp Med 205:2409–2417
43. Osborn EA, Rabodzey A, Dewey CF Jr, Hartwig JH (2006) Endothelial actin cytoskeleton remodeling during mechanostimulation with fluid shear stress. Am J Phys Cell Phys 290:C444–C452
44. Tzima E (2006) Role of small GTPases in endothelial cytoskeletal dynamics and the shear stress response. Circ Res 98:176–185
45. Dudek SM, Garcia JG (2001) Cytoskeletal regulation of pulmonary vascular permeability. J Appl Physiol 91:1487–1500
46. Parker JC, Yoshikawa S (2002) Vascular segmental permeabilities at high peak inflation pressure in isolated rat lungs. Am J Physiol Lung Cell Mol Physiol 283:L1203–L1209
47. Amano M, Chihara K, Kimura K et al (1997) Formation of actin stress fibers and focal adhesions enhanced by rho-kinase. Science 275:1308–1311
48. Roth T, Podesta F, Stepp MA, Boeri D, Lorenzi M (1993) Integrin overexpression induced by high glucose and by human diabetes: potential pathway to cell dysfunction in diabetic microangiopathy. Proc Natl Acad Sci U S A 90:9640–9644
49. Davidson MK, Russ PK, Glick GG, Hoffman LH, Chang MS, Haselton FR (2000) Reduced expression of the adherens junction protein cadherin-5 in a diabetic retina. Am J Ophthalmol 129:267–269
50. Nilsson E, Jansson PA, Perfilyev A et al (2014) Altered DNA methylation and differential expression of genes influencing metabolism and inflammation in adipose tissue from subjects with type 2 diabetes. Diabetes 63:2962–2976